

8.4 THE ROLE OF THE NORTH ATLANTIC THERMO-HALINE CIRCULATION AS A POSSIBLE TRIGGER FOR THE YOUNGER DRYAS OSCILLATION

Jonathan Ariel Forest Byrne
Earth and Space Science Consultant
Rising Sun Consulting
Boston, MA
Byrnejonathan12@gmail.com

Abstract: The Younger Dryas Oscillation (YD) is a member of the Millennial Climate Oscillation (MCO / Dansgaard-Oeschger oscillations (DO) that have occurred during the last 115 ka (kiloannum) The YD developed at approximately 12.8 ka. and was characterized by an abrupt reversal of the de-glaciation that had commenced after the peak of the Last Glacial Maximum (LGM) at 21 ka. This sub-orbital oscillation became amplified as a rapid decrease in surface temperature of 5 c to 10c in the vicinity of the North Atlantic Basin (NAB) over a period of mere decades, followed by warming of equal magnitude. A number of hypotheses have been propounded to explain this abrupt climate change (ACC) event including changes in atmospheric composition (greenhouse gases e.g. CO₂ CH₄ a bolloid impact and ejection of atmospheric aerosols, and a shut down the meridional over- turning (MOD) / thermohaline circulation (THC) in the North Atlantic Basin. In the case of the latter hypothesis, it has been propounded that the outburst of pro-glacial Lake Agassiz released a copious volume of fresh water (FW) into the North Atlantic Basin diminishing the density gradient of the North Atlantic gyre This forcing resulted in ocean-atmosphere coupled radiative cooling of the high latitudes of the NAB due to a significantly reduced poleward advection of warmer subtropical surface water. This paper will investigate the MOD / THC and its role as a trigger for the Younger Dryas event.

1. Overview.

At the height of the Last Glacial Maximum (approximately 21 ka (kiloannum) the Laurentide Ice Sheet (LIC) covered $2 \times 10^7 \text{ km}^2$ of the North American continent, while the Eurasian Ice Sheet (EIC) covered $5.5 \times 10^4 \text{ m}^2$ as ice covered $5 \times 10^6 \text{ m}^2$ of the southern hemisphere. An orbital forced de-glaciation then commenced resulting in the accumulation of glacial melt water in the isostatically depressed southern portion of the Canadian Shield forming pro-glacial Lake Agassiz separate channels (Figure 4). Geologic evidence suggests several outburst episodes that included the Mackenzie, Mississippi and St Lawrence rivers. (Figure 4). The diffusion of fresh water into the North Atlantic Basin, in turn, resulted in fresh water capping hence break down in the thermo-haline, meridional overdriven circulation (THC/MOC)

The end state of the breakdown consisted of a preclusion in the gyre driven meridional transport of subtropical surface water toward polar latitudes. This signal was transmitted and amplified through the terrestrial environment as cooling especially in the vicinity of the Atlantic basin where surface temperatures decreased between 2 – 10 C. This event, identified as the *Younger Dryas Oscillation* (after the arctic tundra flower *Dryas Octepela* that proliferated during this period) spanned approximately 1.3×10^3 years. The Younger Dryas (hence YD) is a member of the numerous Dansgaard Oeschger oscillations that characterized the Holocene.

2. Orbital Forced Climate Change

Second order climate variability (e.g. Dansgaard-Oeschger (Dansgaard, et al. 1984; Oeschger et al. 1984) and Heinrich events (Heinrich H. 1988) are sub-oscillation superimposed on larger scale, orbital driven climate change.

The solar radiation is defined by

$$E = hc / \lambda$$

Where $h = \text{Planck's constant } 6.626 \times 10^{-34} \text{ J / sec}^{-1}$, $c = \text{speed of light } 3 \times 10^{10} \text{ cm}^{-1} \text{ sec}^{-1}$ and λ represents wave frequency per second.

The amount of radiation received at the cross section of the upper terrestrial Atmosphere is defined by

$$I = E (4\pi R^2) / (4\pi r^2)$$

Where $E = \text{radiation at the sun's surface}$, $I = \text{radiation received at the top of the terrestrial atmosphere}$. $R = \text{the sun's radius}$, $r = \text{radial distance between the sun and a the top of the terrestrial atmosphere}$.

Hence the solar constant is calculated as

$$S_0 = E (\text{sun}) (R (\text{sun}) / r)^2$$

where the average value for $S_0 = 1.372 \times 10^3 \text{ W / m}^2 / \text{sec}^{-1}$. However due to the solar angle and coriolis force the actual solar constant is reduced at the terrestrial surface to 374 W / m^2

Oscillations in the solar radiation are (partially) the result of gravitationally forced orbital perturbations. Referred to as the Milankovitch cycles, they are defined as the following 1) *Orbital eccentricity*: Oscillations between circular and more elliptical orbits resulting in shifts in the semi-major axis (where $e = c / a$, and $c = \text{focci}$ and $a = \text{semimajor axis}$). However, with a return frequency of 10^5 and $4 \times 10^5 \text{ yr}$ this cycle represents the lowest impact of the three cycles as a value for $e = 0.05$ will translate to a change in the solar insolation at 65 N of only 0.5 W m^{-2} 2) *Obliquity*: Shifts in the earth's equatorial plane relative to the plane of the ecliptic ranging between 22.5 and 24.5 deg can result in a change in solar insolation at 65 N of approximately 4%, or 17 W m^{-2} (when $e = 0.04$) The return frequency is $4.1 \times 10^5 \text{ yr}$. 3) *Precession* (or "wobble") of the earth's axis produced by the gravitational torque between the earth, moon and sun with can result in change in the solar insolation at 65 N of 8%, or 40 W m^{-2} . The return frequency is $2.6 \times 10^4 \text{ yr}$.

Milankovitch Cycles

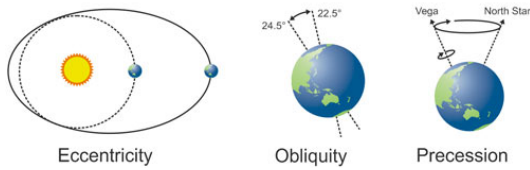


Figure 1. The three oscillations derived from the gravitational interrelationship between the earth, sun and moon,

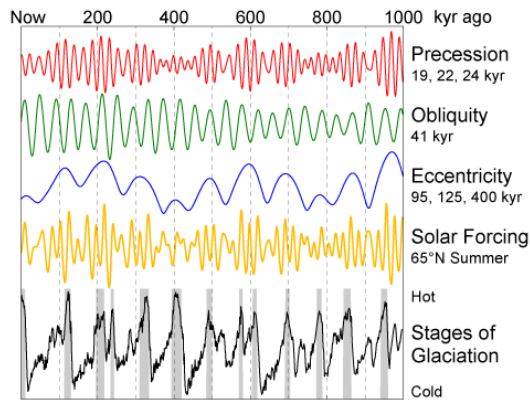


Figure 3: Correlation between Milankovitch cycles, solar forcing at 65°N and glacial oscillations and during the Pleistocene period,

2.1 The Last Glacial Maximum as Antecedent to the Younger Dryas Oscillation.

LIC reached 3×10^3 m over the Canadian Shield. The mass balance and flow velocity of the ice sheet is defined by

$$\partial H / \partial t = -\nabla \cdot \mathbf{H}\mathbf{U} + M$$

where H = thickness, \mathbf{U} = velocity, ∇ is the divergence operator, M = accumulation. The velocity of the ice sheet complies with Glen's Flow Law where ice flow is the product of multiple variables including stress, strain, gravity, ice density, specific heat, temperature and thermal heat flux.

The growth inducing positive feedback loop is represented by the radiative cooling power of the ice sheet. Hence the increase in the R (radius) is defined by the following:

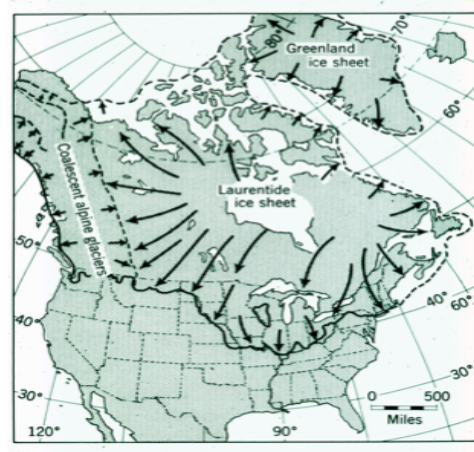


Figure 2: The steady state Laurentide ice flow regime as the ice margin held close to their maximum positions 21 ka – 17 ka (Mayewski et al. 198

$$t + kR^2 = hR$$

where t represents temperature decrease, k represents the cooling coefficient for every 1 degree latitude up to 10 degree, R the growth radius, and h is the $\Delta T / \Delta$ latitude. Positive values for R are maintained when the equilibrium altitude line is collocated with the line for maximum snowfall. (C Brooks 1926) Conversely the decoupling of these two respective boundaries can switch the feedback loop to negative hence reversing the value for R . As the ice sheet expands radially outward the air masses near the center of the becomes more anticyclonic magnifying this decoupling. The end state is a significant snowfall deficit near the center of the ice sheet resulting in the diminution of mass. The diminished mass of the ice sheet, in turn, becomes amplified once orbital (or sub-orbital) forced warming commences.

The retreat / thinning of a marine glacier below sea level is defined by

$$M = M_b + M_h + M_L$$

where M = Mass,

M_b = climatically controlled temperature, M_h = thinning / thickness, and M_L = (the most significant variable) the non-linear dynamic behavior in contrast to the steady state of the of the SMB (Surface Mass Balance)

The transition of the LGM to inter stadial warmth of the Bolling Allerod may have been orbital forced as the phase of the precession cycle i.e. the winter equinox in the northern hemisphere became co-located with perihelion in the earth's orbit thus increased anti-phasing between the seasons. The increase in extremes especially between winter and summer seasonality, in turn, resulted in greater ice / snow amelioration during the summer ultimately reversing the albedo feedback loop from positive to negative. Evidence suggests that the northern hemisphere summers especially around the North Atlantic basin were warmer than summers at present in spite of the more extensive ice cap.

In addition the *Polar Amplification hypothesis* propounds that the polar regions are more sensitive to changes in both orbital (e.g. solar insolation); and suborbital (e.g. greenhouse gas forcing) than lower latitudes. For example, during the LGM ^{18}O (Greenland ice core) indicates a decrease in surface temperatures of between -7 and -20 in the polar regions (Conversely. at present anthropogenic greenhouse gas forcing has increased polar surface temperatures (especially in the N.H.) between 2 and 12 c resulting in a negative value for R for the polar ice cap.

2.3 The Mean Annual Climate Model for the LGM

The mean annual climate at the LGM, as computed by Marsiat and Veldes (2001) and using an Atmospheric General Circulation Model, Siegert and Marsiat showed northern hemispheric synoptic pattern consistent with a positive Arctic oscillation signal (or +AO i.e. a vertical cross section of negative height departures over the Arctic region) with a strong middle latitude zonal flow at 500 hPa curved anticyclonically over the central NAB between 0 – 30 W and 55 – 65 N. Commensurate with this curvature is meridional warm advection forced by a strong pressure gradient between by weak

low pressure and centered over Greenland and a strong high pressure centered over southwest Europe at 50 N / 5 W. The near basin wide thermal ridge signal produced by the warm advection pattern features a steep isothermal gradient change of between +5 – -30 This isothermal gradient, or *thermal ridge* is peripheral to the terminus of both the LIC and EIC along the continental shelf

This thermal ribbon, especially along the east coast of North America is consistent with the modern synoptic signature for polar jet stream dynamics and associate baroclinic disturbances that undoubtedly contributed to the glacial budget,

2.2 Orbital / Sub-Orbital Climate Forcing

Orbital patterns reflect stochastic, unforced processes where orbital insolation acts as trigger with feedback mechanisms and climate thresholds acting as amplifiers to Also model simulations of surface temperature change in the North Atlantic basin associated with a cut off of the THC can cause a substantial change in the Hadley circulation and propagation (Manabe and Stouffer, 1988; Kawatt et al. 1997)

The El Nino / Southern Oscillation, the most significant inter-annual climate signal also contributes to the global energy budget through atmospheric long wave and cloud distribution patterns (Pierrehumbeit and Roca 1998; Pierrehumbeit 1991) In fact any change in the tropics tends to amplify through the entire troposphere due to tight coupling and enforcement by Hadley / Walker circulations.

FW can also be transported from the Atlantic to the Pacific basins through low level wind and precipitation patterns. Also Wind shifts can also affect tropical upwelling, hence subtropical gyre possible leading to a change in heat transport.

transmit the signal throughout the system (Cronin, ****)

For example, fluxes in greenhouse gas dispersion (e.g. CO_2 and CH_4) forced by fluctuations in orbital insolation, coupled with recycling through sources and sinks contribute toward trigger mechanisms and amplification of climate signals and feedback loops.

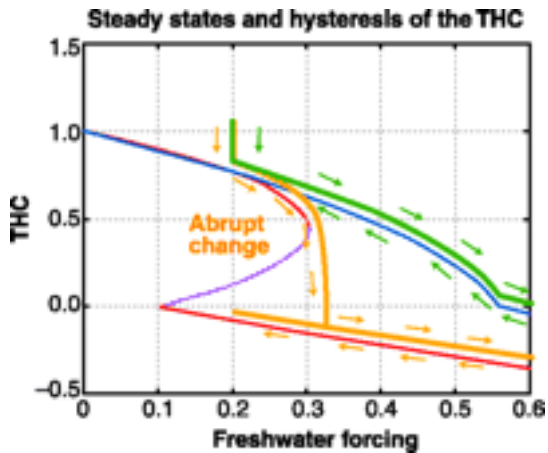


Figure 3. A solution to the Stommel salt advection diagram depicting THC flow (Y axis) in response to FW forcing in Sv (Sverdrups. $1 \text{ Sv} = 10^6 \text{ m}^{-3}$) (x axis) The AMOC operates in two end state equilibrium modes 1) Strong DWF / MOC(upper plot) 2) Weak DWF / MOC and shut off of the THC / MOC (lower plot). The perpendicular plot in the center represents an abrupt convective shutdown, of (or “Welander feedback”). The “tipping point” along the hysteresis loop can be forced with FW values as low as 0.06 Sv (Rhamstorf 1995, 1996, 2002)

3. Lake Agassiz Discharge Event

Based upon the correlation in ^{18}O between Greenland ice cores and LA discharge, Teller and Leverington (2004) estimated a sudden increase in FW discharge of between $2.5 \times 10^3 \text{ km}^3$ and 10^4 km^3 above the mean level outflow level occurred in five distinct stages between 13.5 and 8.2 ka: The Ojibway, Nipigon, Emerson, Moorehead and Lockhart.

Paleo-hydrological reconstruction of glacial lake sediments provide clues for lake drainage history using an array of geochemical methods including oxygen and carbon isotope Proxies (Lewis et al. 1994, Remenda et al. 1994; Buhay and Betcher 1998; Birks et al. 2003)

However an investigation conducted by Rodriguez and Vilks (1994) concluded that Lake Agassiz meltwater did not flow directly into the North Atlantic basin. In fact radio carbon dating of wood indicates onset of the Champlain sea marine episode coincided with the beginning of the YD (Occhietti and

Richards, 2003) a double freshening pulse of Lake Vermont and Lake Condonia followed by a pulse of FW from Lake Agassiz. Discharge is represented as:

$$Q = A \times V$$

where discharge Q is a function of the cross-section of channel A and the flow velocity V . Fisher et al. (2002) calculated that the likely vhe LA outflow through the Athabasca – Clearwater spillway to be $12 \text{ m}^{-1} \text{ s}^{-1}$



Figure 4 Outflow from pro-glacial Lake Agassiz occurred in several stages between 13.5 – 11.4 ka The outflow resulted in a lake level decrease of 100 m

In addition, the tropics e.g. shifts in the ITCZ (Clemel et, al 2001) play a key role in transmitting / amplifying climate change signals on a global level through the re-organization and distribution of water vapor.(***)

3.1 Model Experiments Of The THC/MOD

Experiments conducted by Ganapolski and Rahmstorf (2002) using the CLIMBER – 2 model simulated both DO and H events by introducing FW forcing of between $0.015 - 0.045 \text{ Sv}$ into the Nordic Sea under glacial boundary conditions which resulted in a DO type signal. **Additional** experiments where FW forcing of 0.15 (the approximate volume of FW outflow from the LIC) resulted in a complete shutdown of the NA THC as it did not return until the forcing was turned off.

Inter-model comparison studies of modern climate-ocean conditions (Rahmstorf et al. 2005) , eleven of which were of intermediate complexity with a FW influx of 0.05 Sv resulted in a wide range MOC climate sensitivity responses but a qualitative

agreement about hysteresis behavior to support Stommel salt advection model.

Also relatively small amounts of FW forcing e.g. 0.06 Sv on high latitudes of the NAB resulted in a shutdown of NADW (North Atlantic Deepwater) and a change in climate equilibrium
 Rahmstorf (1995), Ganopolski and Rahmstorf (2002); Manabe and Stouffer (1995, 1997). (1 Sv = 10^6 m^2 = total global river outflow)

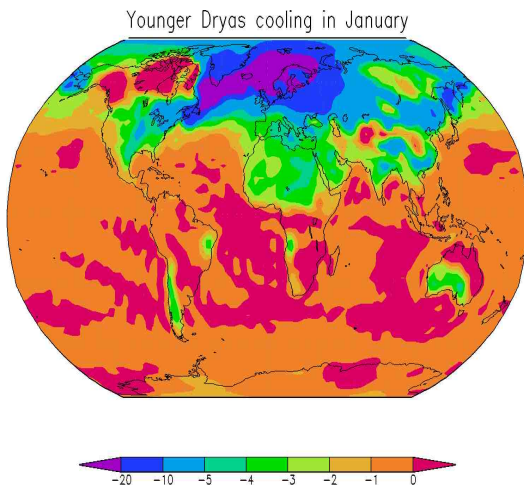


Figure 5. Negative anomalies in SST resulting from FW forced cooling in the high latitudes of the NAB and surrounding terrestrial regions; and widespread antiphased positive anomalies in the SH

4 Alternative Trigger Hypotheses For The YD

Firestone et al.(2005) has proposed a terrestrial impact as a trigger for and the YD oscillation based upon diamond deposits discovered globally. This hypothesis is consistent with the model for boloid impacts as a trigger for abrupt climate change (e.g. the K-T at appx 6500 ka that resulted in mass extinctions hence terminating the "dinosaur" era). In this model the copious ejection of atmospheric aerosols diminish terrestrial solar insolation triggering rapid global cooling. However this hypothesis remains controversial and subject to further investigation.

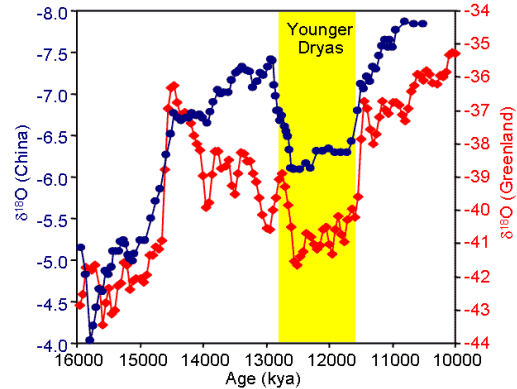


Figure 4: Decrease in O during YD where $\Delta O = -1\%$ for every $\Delta T = -1.5 \text{ c}$

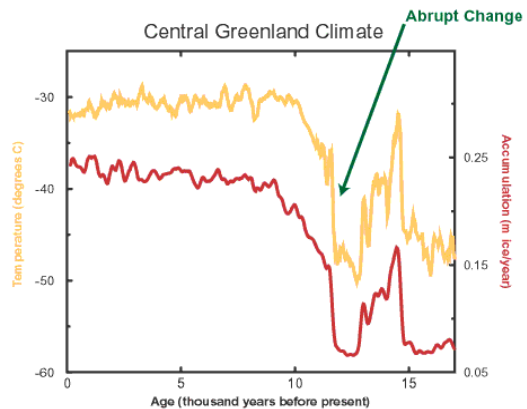


Figure 6. YD signal reflected by the correlation between temperature (Y1 – red) and ice accumulation / yr (Y2 yellow)

5. Evidence for Alternative LA Outflow During the YD.

Many unresolved issues remain around the routing of LA discharge. Changes in salinity during the middle of the Champlain Sea episode lead Rodriguez and and Vilks (1999) to the conclusion that melt water did not flow into the NAB at the onset of the YD (as originally proposed by Broecker) According to their investigation the radio carbon of wood indicates that the onset of the Champlain Sea episode actually coincided with the YD. Occhietti, Richard (2003) concluding that Lake Condon and Lake Vermont drained at this time.

6. Marine Evidence for YD

Bond and Lotti, 1995; Bond et al. 1999; Rasmussen et al. (1996, 1997, 2000) found evidence for 15 DO cycles during the past 58 ka in NAB marine sediment. For example cooler SST, reduced NADW, increased ice cover were reflected in benthic foraminiferal assemblages especially the cold adapted *N. Pachyderma*. during the peak cooling of the stadial periods. Conversely interstadial periods were dominated by warm foraminiferal assemblages signaling strong meridional overturning and NADW formation. Sachs and Lehman (1999) used alkenone paleothermometry to measure a mean 3.1 C SST range (1.7 – 5.3) in the subtropical Sargasso Sea during 12 DO events

In addition, comparison of $\delta^{18}\text{O}$ and deuterium (δD) isotopes provides a D excess that serves as a measure of the evaporation temperature of the moisture that eventually falls in ice. Therefore δD is closely tied to SST and humidity in the source area of evaporation Stenni et al. (2001), Stenni et al. (2003)

6.1 Greenland / Antarctic Synchronicity

Antarctic oscillations appear more sinusoidal in contrast to the spikiness of Greenland (EPICA, Community member 2004, 2006, Jouzel et al. 2007) However CO_2 N_2O CH_4 found within trapped ice core bubbles in both Greenland and Antarctic ice signal a global manifestation of DO events including stadial and interstadial temperature fluctuations. This signal, in turn, supports the ocean teleconnection the NH and Antarctic via a bi-polar 'see saw' mechanism.

Cooling in the N.H. occurred within a few decade long steps, as warming of 8 c occurred in one decade long step; snow accumulation doubled within three years, and methane rose by 50% / 100 yr toward the end of the YD (Chappellaz et al. 1997, Severinghaus et al. 1998, Brook et al. 1999)

7. Summary

Climate oscillation consist of a complex, spatial-temporal interaction between stochastic and non-linear forcings that are both internal and external to the terrestrial environment. First order climate oscillations are externally forced by earth-sun moon geometry i.e. the Milankovitch cycles that impact the magnitude and distribution of solar radiation. First order climate oscillations are more symmetric and sinusoidal and are associated with time resolutions ranging from 26 ka (precession) to a maximum of 400ka for orbital eccentricity. (Additional externally forced, first order climate oscillations may be considered including variations in solar luminosity, cosmic rays, interstellar gas and dust but are beyond the scope of this paper.)

Second order climate oscillations, or MCO are also composed of complex interrelationships between multiple internal forcings. Such forcings include atmospheric composition e.g. greenhouse gases e.g. CO_2 and methane; terrestrial feedbacks e.g. albedo, hydrologic cycles, annular modes e.g. AO, AAO, ENSO; and the THC/ MOC responsible for ocean-atmosphere coupled thermal advection patterns. Millennial Climate Oscillations are high time resolution events ranging from 1-2 ka to mere decades. MCO are more asymmetric i.e. "spikey", stepwise, with a 2% variation between "spikes" and troughs. MCO have also been defined as DO and Heinrich events and represent up to twenty four oscillations that have occurred during the last 58 ka, with a return frequency of between 1.5 and 2.5 ka

In addition, the cross-linking between forcings of both first and second order climate oscillations cannot be underscored. As aforementioned during the LGM, orbital induced de-glaciation at 21 ka may have triggered the YD through the accumulation of glacial melt water within the isostatically depressed Canadian shield then ultimate outburst of pro-glacial lake Agassiz into both the Pacific and Atlantic basins via three primary channels. The FW forcing that resulted from this outburst forced a shut down of the THC /MOC of the NAB. The bi-

hemispheric synchronicity of especially ^{18}O , and methane signatures (as supported by GRIP and EPICA data) suggest that this signal became amplified globally through a rapid decrease in surface temperatures up to 10 c especially in proximity of the Atlantic basin, and its impact on atmospheric circulation patterns, annular modes including monsoon oscillations in India and South America, Hadley cells and the ITCZ>

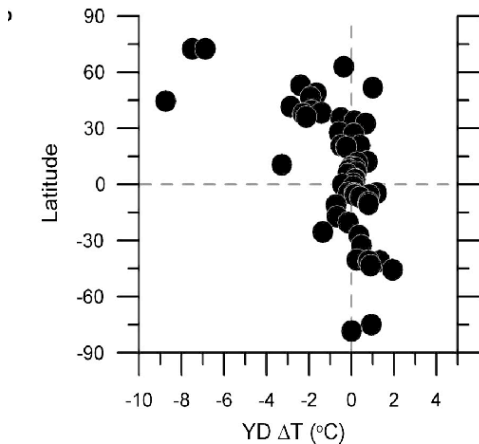


Figure 8. Epicenters of Maximum cooling during the YD oscillation

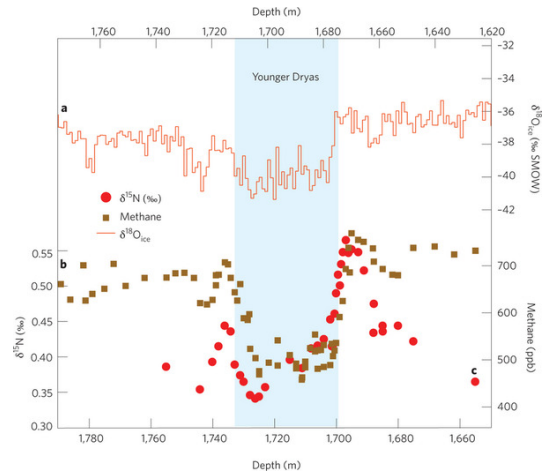


Figure 7. depicts the correlation between temperature and atmospheric methane levels. Y (left) = $\delta^{15}\text{N}$ (%) red plot. Y (lower right) = δ methane (green plot) δ (ppb) Y (upper right) $^{18}\text{O}_{\text{ice}}$ Upper plot; X = snow depth (m)

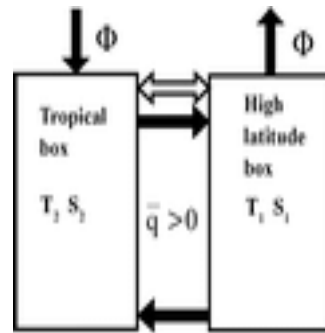


Figure 9. Stommel Diagram: T= temperature, S = salinity q = velocity flux, Φ = FW forcing. Tropical box = increased T, decreased FW due to evaporation; High Latitude box = decreased T, Increased FW forcing due to reduced evaporation.

ID 209387
PS 869782

8. References

Alley, R.B. 2000 The Younger Drayas cold interval as viewed from central Greenland. *Quarternary Science Reviews* 19:213 -226

Alley, R. B. and D.R. MacAyeal. 1994. Ice rafted debris associated with binge / purge oscillations of the Laurentide Ice Sheet. *Paleoceanography* 9:503 - 511

Alley, R. B. and P.U. Clark. 1999: The deglaciation of the Northern Hemisphere: A global perspective. *Annual Reviews of Earth and Planetary Sciences* 27:149-182

Bond, G. , W. Showers, M. Chesby, Lotti, I. Hajdas, and Bonani. 1997. A pervasive millennial scale cycle in North Atalantic Holocene and Glacial Climates. *Science* 278 1257 - 1266.

Broecker, W.S. *The Great Ocean* Conveyer 2010 Princeton University Press

Broecker, W.S.1998. Paleocean circulation during the last deglaciation: A bipolar see-saw? *Paleoceanography* 13:119-121

Broecker, W. S. *The Glacial World According to Wally* 2nd Edition. Eldigo Press, Lamont-Doherty Earth Observatory of Columbia University, Palisides, NY.

Broecker, W.S., and G.H. Denton. 1989. The role of ocean-atmosphere reorganization in glacial cycles. *Geochemica et Cosmochi,ica Acta* 53:2465-2501

Brooks C. E. P. 1926: *Climate Through The Ages* Dover Press

Cronin, T. M. 1991 *Principles in Paleoclimatology*. Columbia University Press, New York

Fanning, A. F., and A. J. Weaver. 1997 Temporal -geographic influences on the North Atlantic conveyor: Implications for the Younger Drayas *Paleoceanography* 12:307 -320

Manabe, S., and R.J. Stouffer. 1985. The influence of continental ice sheets on the climate of the ice age. *Journal of Geophysical Research* 90: (C2) :2167 - 2190.

Rahmstorf, S. 1994 Rapid Climate transitions in an ocean-atmosphere coupled model. *Nature* 378: 82-85

Rahmstorf, S. 1996. On the freshwater forcing and transport of the North Atlantic thermohaline circulation. *Climate Dynamics* 12:799 - 811

Stommel, H. Thermohaline convection within two stable regimes of flow. *Tellus* 13:224 - 230